in "Simulation Studies in Condensed Matter Physics: Recent Developments" (Springer 1988)

Classical Spin Dynamics in the Two-Dimensional Anisotropic Heisenberg Model

G. M. Wysin, M. E. Gouvea*, A. R. Bishop
Los Alamos National Laboratory
Los Alamos, NM 87545 USA

F. G. Mertens
Physics Institute, University of Bayreuth
D-8580 Bayreuth, Fed. Rep. of Germany

ABSTRACT

Properties of vortices and dynamic correlation functions have been studied for the two-dimensional classical ferromagnetic Heisenberg model with easy-plane anisotropy, as a function of the anisotropy parameter $\lambda = J_z/J_x$. Continuum limit equations of motion exhibit two types of static vortex solutions, with and without out-of-plane spin components. We have studied numerically the stability of these solutions and have found that for $\lambda \lesssim 0.7$ only the planar vortex (zero out-of-plane spin components) is stable, and for $\lambda \gtrsim 0.8$ only the vortex with nonzero out-of-plane spin components is stable. Approximate spin configurations for non-zero-velocity vortices are presented. A vortex ideal gas phenomenology is used to calculate the dynamic correlation function $S(\vec{q},\omega)$. Above the Kosterlitz-Thouless transition temperature, the calculation predicts a Gaussian central peak for the out-of-plane correlations and a squared Lorentzian for the in-plane correlations. These results are compared with results of a Monte Carlo-Molecular Dynamics simulation.

1. INTRODUCTION

Quasi-two-dimensional (2D) spin systems provide challenging realizatons of models ideally suited for large-scale numerical simulations of dynamical behavior. Model Hamiltonians including anisotropic (easy-plane) exchange and possibly in-plane symmetry breaking are believed to describe materials of current experimental interest, such as $BaCo_2(AsO_4)_2$, Rb_2CrCl_4 [1,2] and $CoCl_2$-GIC [3]. In a classical description, the models support interacting nonlinear domain walls, vortices, and spin waves, and therefore can be used to test theories for the stability, energy dispersion, and interactions between these excitations. Continuum limit theory can be used as a guide, and can be compared with numerical simulations on finite lattices, where the effects of discreteness may modify the dynamics. These can be compared with experimental results, especially inelastic neutron scattering data. The low-frequency long-wavelength dynamic correlations are particularly relevant as signatures for topological excitations, such as vortices and domain walls.

The model Hamiltonian we consider is the easy-plane anisotropic Heisenberg ferromagnet with nearest neighbor interactions:

$$H = -J \sum_{(i,j)} (S_i^x S_j^x + S_i^y S_j^y + \lambda S_i^z S_j^z). \qquad (1)$$

The exchange parameter is $J > 0$, and $0 \le \lambda \le 1$ measures the degree of anisotropy. For the XY model ($\lambda = 0$), the system is expected to undergo a Kosterlitz-Thouless (KT) topological phase transition at a finite temperature T_{KT} [4]. Static spin-spin correlations are expected to change from power law to exponential as the temperature T is raised above T_{KT}, due to a finite density of vortex-antivortex pairs becoming unbound. For $T > T_{KT}$, we therefore expect there will be a low density of free vortices interacting weakly with one another, in a background spin field of the remaining bound pairs and renormalized spin waves [5]. This is reminiscent of the soliton ideal gas picture for 1D magnets [6]. Phenomenologically, we can determine the vortex ideal gas contribution to the dynamic structure

function $S(\vec{q},\omega)$, as in Mertens et al. [7], for in-plane and out-of-plane correlations. The theory includes phenomenological parameters that are temperature dependent, including an rms vortex velocity $\overline{u}$, and a correlation length ξ equal to half the mean vortex-vortex separation. We will also assume a vortex number density $n_v \simeq (1/2\xi)^2$. As in the 1D soliton models, a central peak ($\omega \simeq 0$) in $S(\vec{q},\omega)$ is expected, relating to the presence of zero-velocity coherent nonlinear structures (i.e., vortices). These results will also apply to nonzero-λ cases; T_{KT} decreases very slowly with λ until λ is very near 1 [8]. However, the out-of-plane correlations might be expected to be modified with increasing λ. This depends on details of the λ-dependence of the out-of-plane spin configurations for moving vortices, which we consider below.

The total $S(\vec{q},\omega)$, due to all excitations and their interactions, can be determined from numerical simulations using a combined Monte Carlo-Molecular Dynamics (MC-MD) approach [9]. A (microcanonical) MD integration of equations of motion is performed, using initial configurations generated by a MC simulation. Comparisons of the phenomenology with numerical experiments and laboratory experiments must allow for effects of nonlinear interactions between the interactions. In particular, higher order spin wave processes also can contribute to the central peak; we are presently considering this problem.

We have three primary goals here. First, we consider the dynamics of an isolated vortex, in the continuum limit and numerically on a lattice, to determine the energy dispersion, stability, and approximate out-of-plane spin configuration. This is done for stationary and moving vortices. Second, the vortex ideal gas phenomenology is reviewed, and the vortex spin configurations are used to predict the free vortex contributions to $S(\vec{q},\omega)$. Third, we compare the phenomenological predictions with numerical simulations on a square lattice, specifically for the central peak (CP) properties of the XY model.

2. CONTINUUM LIMIT VORTEX PROPERTIES

For the continuum classical dynamics of Eq. 1, we define the in-plane spin field $\phi(\vec{r})$ and out-of-plane spin field $\theta(\vec{r})$ by

$$\vec{S}(\vec{r}) = (\cos\theta\cos\phi,\ \cos\theta\sin\phi,\ \sin\theta), \tag{2}$$

where $\vec{r} = (r,\varphi)$ in polar coordinates. Assuming small spatial derivatives (for example, a $\partial\theta/\partial r \ll 1$, $(a/r)\,\partial\theta/\partial\varphi \ll 1$, a = lattice spacing), the continuum equations of motion are [10, 11]

$$\dot{\theta} = \cos\theta\,\nabla^2\phi - 2\sin\theta\,\vec{\nabla}\theta\cdot\vec{\nabla}\phi, \tag{3}$$

$$\dot{\phi}\cos\theta = [2\delta - (\delta\,|\nabla\theta|^2 + |\nabla\phi|^2)/2]\sin 2\theta - (1-\delta\cos^2\theta)\nabla^2\theta, \tag{4}$$

where the unit of time is $\hbar/JS$, and

$$\delta = 1 - \lambda\ . \tag{5}$$

The Hamiltonian contains terms due to θ and ϕ gradients, as well as an anisotropy term (we set a = 1):

$$H = \frac{JS^2}{2}\int d^2r\ \{(1-\delta\cos^2\theta)\,|\nabla\theta|^2 + \cos^2\theta\,|\nabla\phi|^2 + 4\delta\sin^2\theta\}. \tag{6}$$

For static configurations, $\dot{\theta} = \dot{\phi} = 0$ and Eq. 3 admits the solution for a vortex (or antivortex) at the origin:

$$\phi = \pm\tan^{-1}(y/x) + \phi_0, \tag{7}$$

where ϕ_0 is an arbitrary constant. The corresponding out-of-plane component can

have two distinct configurations. First, there is a "planar" solution, with $\theta_{pl} = 0$, and energy $E_{pl} = \pi JS^2 \ln (R/r_o)$, where R is the system size and $r_o \simeq a$ is a vortex core cut-off for the radial integration. The second solution involves nonzero out-of-plane spin components, with asymptotic values

$$\theta_{out} \simeq A(r_v/r)^{1/2} e^{-r/r_v}, \quad r \to \infty \tag{8}$$

$$\theta_{out} \simeq \pi/2 - \tilde{A}\, r/r_v , \qquad r \to 0 \tag{9}$$

$$r_v = \frac{1}{2} \left(\frac{\lambda}{1-\lambda}\right)^{1/2} \tag{10}$$

If we match the asymptotic functions at $r = r_v$, then

$$A = \pi e/5 \text{ and } \tilde{A} = 3\pi/10 . \tag{11}$$

The energy E_{out} is a function of λ and r_o. The decay of θ_{out} for large r is characterized by a vortex radius r_v. For the XY model, $r_v = 0$, and the out-of-plane solution degenerates to the planar solution. For nonzero λ, relative stability is determined by $E_{out}-E_{pl}$. However, this difference is very sensitive to the value of r_o. To compare with simulations on a square lattice, $r_o \simeq a$, but it may be more appropriate to use $r_o \simeq a/\sqrt{2}$ because this is the smallest r to a lattice site for a vortex centered in a unit cell. Alternatively, the stability can be examined directly on a discrete lattice by numerical means.

For the XY model, the out-of-plane vortex correlations must derive from moving "planar" vortices, which can have nonzero out-of-plane components. An approximate traveling wave solution to Eq. 4 can be found by assuming $\sin\theta \ll 1$ and $(\vec{r}-\vec{u}t)$ time dependence, giving

$$\sin\theta \simeq \frac{\vec{u} \cdot \hat{e}_\varphi r}{1-4r^2} , \tag{12}$$

where $\hat{e}_\varphi$ is the azimuthal unit vector.

The spin profile is proportional to the velocity. The angular dependence on $\hat{e}_\varphi$ is to be expected--the out-of-plane profile necessarily cannot be isotropic in φ if we want the profile to define a distinct direction for the velocity. However, we see that Eq. 12 is discontinuous and diverges at $r = 1/2$; retaining the neglected nonlinear terms presumably would suppress the divergence and force $\sin\theta$ to cross zero near $r = 1/2$. For arbitrary λ, asymptotic solutions for a moving planar vortex are consistent with Eq. 12;

$$\theta \simeq \vec{u} \cdot \hat{e}_\varphi r, \qquad r \to 0, \tag{13}$$

$$\theta \simeq \frac{-\vec{u} \cdot \hat{e}_\varphi}{4\delta} \frac{1}{r} , \qquad r \to \infty. \tag{14}$$

Whether the asymptotic $r \to 0$ solution is relevant for vortices on a lattice is questionable; the continuum "solution" varies too rapidly near $r = 1/2$ to justify the assumption of small spatial derivatives. We consider this question and vortex stability using numerical simulation.

3. VORTEX MOTION ON A LATTICE

For numerical simulations, the discrete equations of motion are

$$\dot{\vec{S}}_i = \vec{S}_i \times \vec{F}_i - \epsilon\, \vec{S}_i \times (\vec{S}_i \times \vec{F}_i) , \tag{15}$$

$$\vec{F}_i = J \sum_{(i,j)} (S_j^x \hat{x} + S_j^y \hat{y} + \lambda S_j^z \hat{z}). \qquad (16)$$

The sum on j is only over the nearest neighbors of i. The parameter ϵ is the strength of a Landau-Gilbert damping, which was included for testing vortex stability and for damping out spin waves generated from non-ideal initial conditions. Neumann boundary conditions were used for simulating single vortices; periodic boundary conditions were used for vortex-antivortex pairs. The equations for the xyz spin components were integrated using a fourth order Runge-Kutta scheme with a time step of 0.04 (using time unit $\hbar/JS$). Conservation of energy and spin length served as checks of numerical accuracy (to about 1 part in 10^5). Single vortex motion was studied on a 40 x 40 square lattice; vortex-antivortex pair motion was studied on a 100 x 100 square lattice.

The stability of static planar vortices was tested by using Eq. 7 as initial condition, with $\theta = 0$, centered in a unit cell. The time evolution was followed to $t = 400$, with damping $\epsilon = 0.1$. For $\lambda \lesssim 0.7$, the planar vortex was found to be stable; a small decrease in energy occurred due to small changes in the boundary spin configuration, but the out-of-plane component remained zero everywhere. For $\lambda \gtrsim 0.8$, however, a nonzero out-of-plane component developed after $t \simeq 100$, and relaxed into configurations as in Fig. 1, approximately described by Eq. 8 and 9 for the out-of-plane vortex. These simulations were also repeated using the out-of-plane vortex as initial condition. Again, we found that for $\lambda \lesssim 0.7$ the planar vortex is the stable configuration and for $\lambda \gtrsim 0.8$ the out-of-plane vortex is the stable configuration

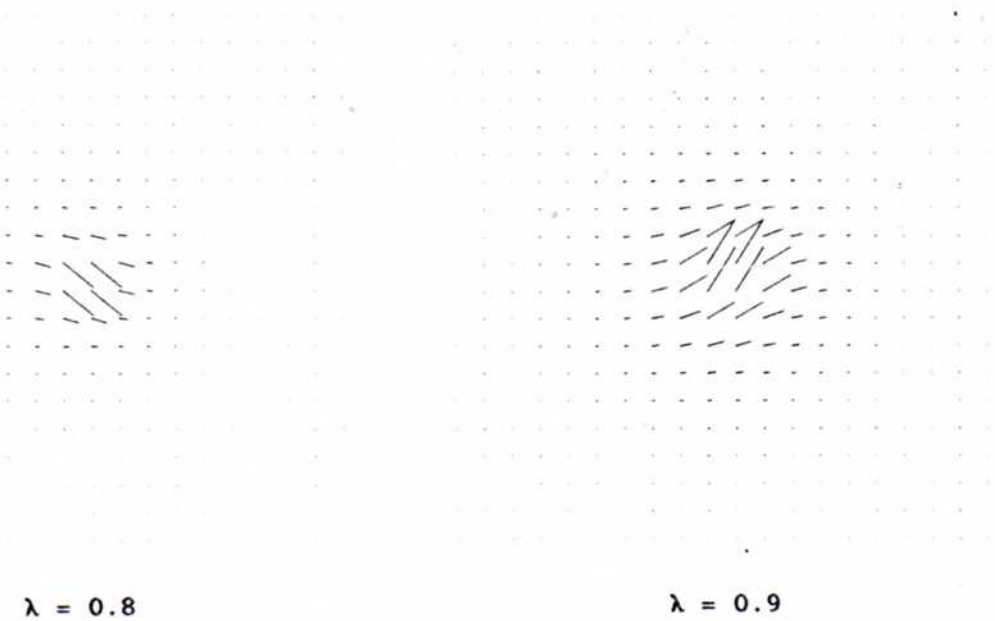

$\lambda = 0.8$ $\lambda = 0.9$

Fig. 1. Single vortex out-of-plane angles θ, after integration for 400 time units starting from a planar vortex ($\theta = 0$). The lengths of the lines are proportioned to θ; the angles from the horizontal axis are θ.

Some insight about moving vortex profiles can be obtained by using static planar vortex-antivortex pairs as initial condition. With $\epsilon = 0.1$, it is found that the pairs move easily toward each other for $\lambda \gtrsim 0.8$. For $\lambda \lesssim 0.7$, however, the attraction is considerably weaker and falls off strongly with distance. An instantaneous configuration is shown in Fig. 2. The azimuthal dependence of the out-of-plane component is clear. There is no sign change in $\sin\theta$ as a function of r. It should be noted that the vortex motion is not along the line connecting the centers, but includes a net drift in the orthogonal direction as well [5].

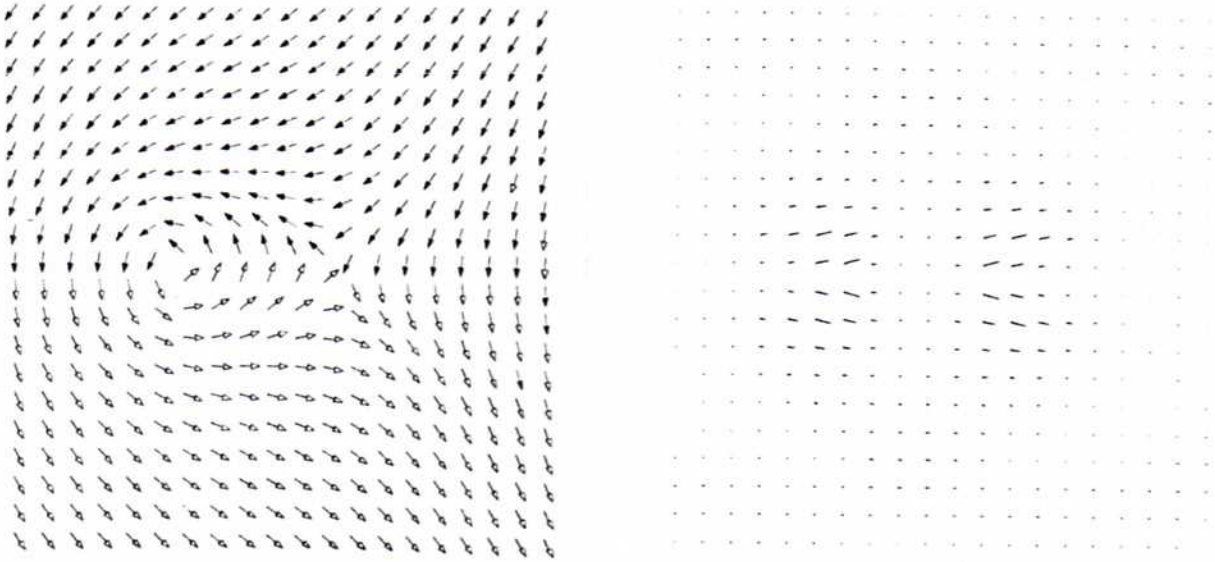

Fig. 2. Vortex-antivortex pair motion for $\lambda = 0.7$, at $t = 15$, starting from a planar pair at $t = 0$ ($\theta = 0$). A 20 x 20 segment of the 100 x 100 lattice simulated is shown. Note the dependence of θ on the azimuthal coordinate for each vortex.

We have also tested profiles for isolated moving vortices without damping. The XY planar vortex, Eq. 12, is not found to be a good traveling wave solution. However, if we modify the r-dependence to $\sin\theta \sim (1-e^{-Br2})/r$, which does not change change sign, then we find that fairly stable moving profiles can be obtained. The details of the small-r dependence of θ still need to be clarified.

4. VORTEX IDEAL GAS PHENOMENOLOGY

The correlations in a dilute gas of free vortices with average separation 2ξ and with a Maxwellian velocity distribution with rms velocity $\bar{u}$ were considered in Mertens et al. [7]. Based on the single vortex stability regimes, we expect that the out-of-plane correlations will be determined by moving planar vortices for $\lambda \lesssim 0.7$ or by out-of-plane vortices for $\lambda \gtrsim 0.8$. Using the large r asymptotic solutions, we can predict the small-wavevector behavior of $S(\vec{q},\omega)$. Assuming incoherent scattering of the vortices, the out-of-plane space-time correlation function is

$$S_{zz}(\vec{r},t) = n_v S^2 \int d^2R \int d^2u\, P(\vec{u})\, \sin\theta(\vec{r}-\vec{R}-\vec{u}t)\, \sin\theta(\vec{R}), \qquad (17)$$

where n_v is the free vortex density and $P(\vec{u})$ is the Maxwell-Boltzmann velocity distribution. For $\lambda \lesssim 0.7$, and using Eq. 14 for θ for moving planar the vortices, space-time Fourier transform of Eq. 17 is

$$S_{zz}(\vec{q},\omega) = \frac{S^2}{32\sqrt{\pi}\delta^2} \frac{n_v \bar{u}}{q^3} e^{-(\omega/\bar{u}q)^2}, \qquad \lambda \lesssim 0.7 \qquad (18)$$

Similarly, for $\lambda \gtrsim 0.8$, the vortex contribution to $S_{zz}(\vec{q},\omega)$ is found using Eq. 8 for θ for out-of-plane vortices, and we find

$$S_{zz}(\vec{q},\omega) = \frac{S^2}{4\pi^{5/2}} \frac{n_v}{\bar{u}} \frac{|f(q)|^2}{q} e^{-(\omega/\bar{u}q)^2}, \qquad \lambda \gtrsim 0.8 \qquad (19)$$

with vortex form factor for $qr_v \ll 1$,

$$f(q) \simeq \pi^{3/2} A r_v^2 \left[1 - \frac{15}{16}(qr_v)^2 + \frac{945}{4 \cdot 16^2}(qr_v)^4 - \cdots\right]. \qquad (20)$$

In both cases there is a Gaussian central peak with width $\Gamma_z = \bar{u}q$. This reflects the assumption of a Maxwellian velocity distribution. The integrated intensities are

$$I_z^{pl} = \frac{S^2}{32\delta^2} \frac{n_v \bar{u}^2}{q^2}, \qquad \lambda \lesssim 0.7, \qquad (21)$$

$$I_z^{out} = \left(\frac{S}{2\pi}\right)^2 n_v |f(q)|^2, \qquad \lambda \gtrsim 0.8. \qquad (22)$$

The small-q divergence of Eq. 21 can be removed by taking into account the finite system size or other similar cutoffs.

For the in-plane correlations, a different approach is needed because the in-plane spin components have no Fourier transform and they are globally sensitive to the presence of vortices. A vortex passing between 0 and r breaks the topological long range order in cos ϕ, diminishing the correlations and changing cos ϕ by a factor of -1. The vortices behave similarly to 2D sign functions. Carefully counting the number of vortices passing between 0 and r in time t leads to [7]

$$S_{xx}(\vec{r},t) \simeq \frac{S^2}{2} \exp\{-[(r/\xi)^2 + (\gamma t)^2]^{1/2}\}, \qquad (23)$$

$$\gamma \equiv \sqrt{\pi}\, \bar{u}/2\xi \qquad (24)$$

Taking the space-time Fourier transform leads to a squared Lorentzian central peak

$$S_{xx}(\vec{q},\omega) \simeq \frac{S^2}{2\pi^2} \frac{\gamma^3 \xi^2}{\{\omega^2 + \gamma^2 [1 + (\xi q)^2]\}^2}. \qquad (25)$$

The CP width and integrated intensity are

$$\Gamma_x \simeq \frac{[\pi(\sqrt{2} - 1)]^{1/2}}{2} \bar{u}\xi^{-1} [1 + (\xi q)^2]^{1/2}, \qquad (26)$$

$$I_x \simeq \frac{S^2}{4\pi} \frac{\xi^2}{[1 + (\xi q)^2]^{3/2}}. \qquad (27)$$

These results can be compared with the MC-MD simulation, for the XY model. We used a 100 x 100 lattice with periodic boundary conditions, allowing access to q $\simeq$ 0.02 (π/a). First, an MC algorithm of 10^4 steps per spin was used to produce three equilibrium configurations at a desired temperature. These were used as initial conditions for MD using 4th order Runge-Kutta time integration with time step 0.04, sampling time N_S x 0.04, and total integration time 512 x N_S x 0.04. The sampling interval N_S = 4 - 32 depending on the wavevectors of interest. A Gaussian window function was applied to $S(\vec{q},t)$ before using an FFT algorithm for the time Fourier transform. $S(\vec{q},\omega)$ was averaged over the three initial conditions.

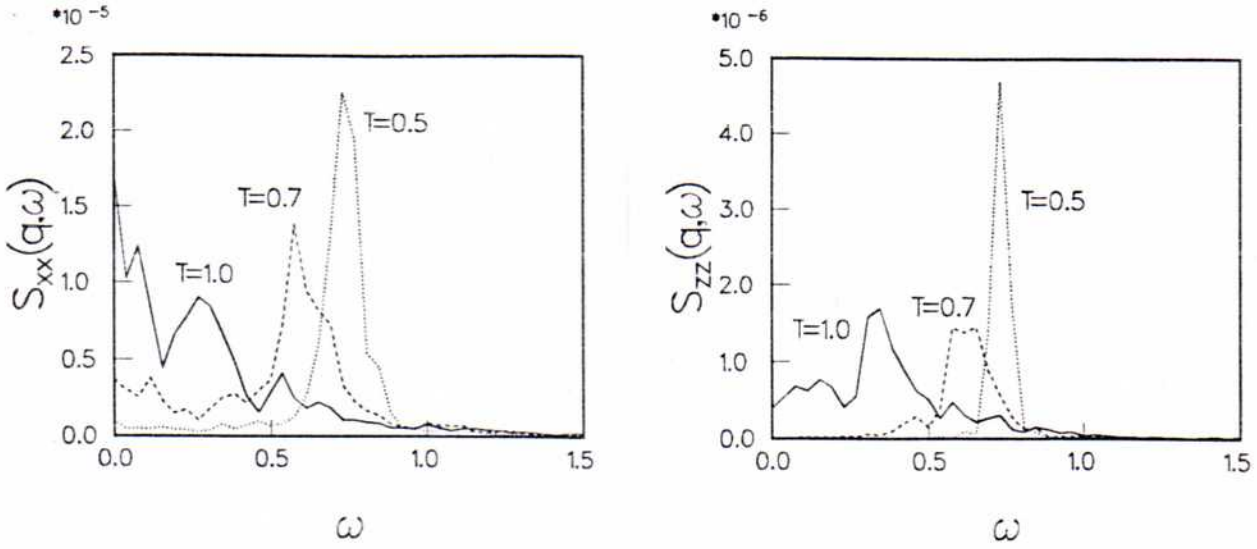

Fig. 3. Results from MC-MD simulations of the XY model on a 100 x 100 lattice, for $\vec{q}$ = (0.10, 0.10) π/a, for a) in-plane correlations and b) out-of-plane correlations. Spin wave softening and development of central peak intensity are seen with increasing temperature.

Typical data are shown in Fig. 3 for three temperatures, where $T_{KT} \simeq 0.8$ J. In-plane as well as out-of-plane spin wave peaks are seen to soften as T is increased towards T_{KT}. Additionally, CP intensity develops. Spin wave frequencies determined from $S(\vec{q},\omega)$ are shown in Fig. 4

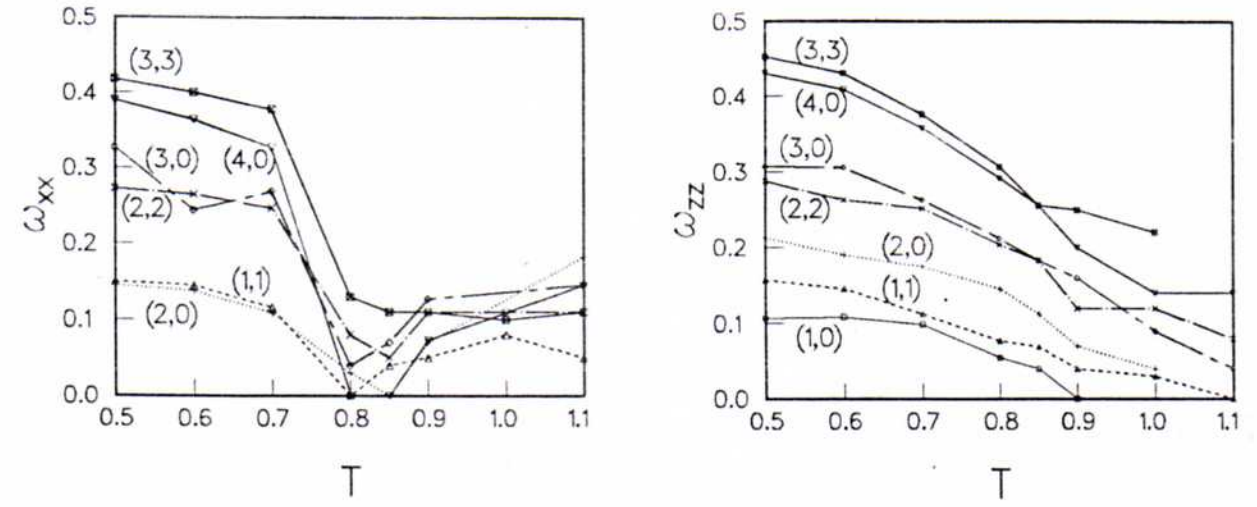

Fig. 4. Spin wave frequencies for the XY model, for q's in units of (1/50) (π/a), as functions of temperature (with J = 1), determined from a) in-plane correlations $S_{xx}(\vec{q},\omega)$, and b) out-of-plane correlations $S_{zz}(\vec{q},\omega)$. The frequencies for $T \gtrsim 0.8$ are crude estimates, especially for ω_{xx}; the softening of ω_{xx} is much stronger than for ω_{zz}.

Estimates (upper limits) of numerical CP widths and intensities are shown in Figs. 5 and 6 for T = 1.0. Agreement with the phenomenology is very good, using u and ξ as adjustable parameters. Fitting Γ_x to Eq. 26 gives $\bar{u} = 0.9$ and $\xi/a = 3.0$ (Fig. 6). Using these values in Eq. 21 gives $I_z = 7 \times 10^{-4}/q^2$; for small q this is larger than the MC-MD calculation of I_z by a factor of 2 (Fig. 5). It is not clear whether finite site corrections for small q are responsible for this difference. It is encouraging that the orders of magnitude are comparable, although the MC-MD data for I_z do not appear to vary as $1/q^2$. Multi-spinwave and other effects due to vortex-vortex and vortex-spinwave interactions may also be responsible for modifying the out-of-plane CP intensity to lower values than predicted for small q. Alternatively, it is probable that part of the in-plane width is due to multi-spinwave processes, and by fitting the observed Γ_x to Eq. 26, we effectively underestimate the vortex-vortex separation 2ξ and thus overestimate the vortex density. This would then result in a predicted out-of-plane intensity due to vortices that is too large. Investigation of these effects will be important for more precise comparisons.

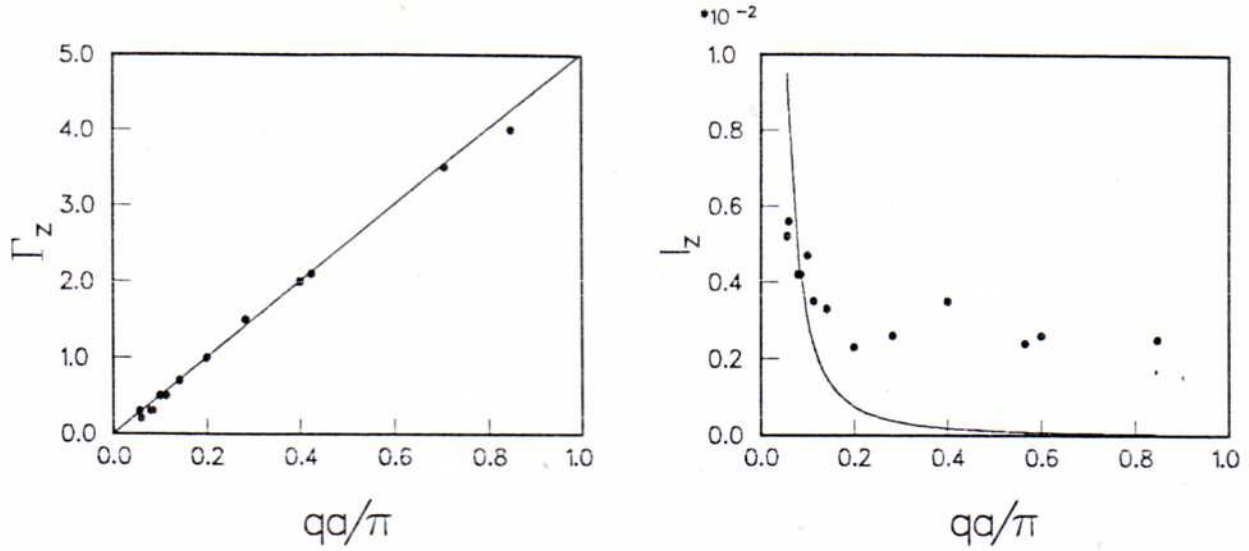

Fig. 5. Central peak properties of $S_{zz}(\vec{q},\omega)$ for the XY model at T = 1.0. In a) we show estimates of the CP width Γ_z from MC-MD data and compare with $\Gamma_z = \bar{u}q$ using $\bar{u} = 1.6$. In b) we show estimates of the CP intensity I_z from MC-MD data and compare with $I_z = 3 \times 10^{-4}/q^2$ (c.f. Eq. 21).

5. CONCLUSIONS

We have made continuum and discrete numerical calculations for classical vortex dynamics in a 2D ferromagnet, for the microscopic single vortex behavior and for the collective behavior of a finite system in equilibrium. From simulations on a square lattice, the planar ($\theta = 0$) static vortex predicted in continuum theory is stable only for $\lambda \lesssim 0.7$, and the out-of-plane static vortex is stable only for $\lambda \gtrsim 0.8$. Therefore, for $\lambda \lesssim 0.7$, out-of-plane correlations due to vortices should be determined by the velocity-dependent out-of-plane spin components of moving planar vortices. Using a large-r asymptotic expression for a moving planar vortex, we have calculated $S(\vec{q},\omega)$ within an ideal vortex gas phenomenology. The phenomenology gives a fairly good description of the central peak behavior of the XY model above T_{KT}, as found in MC-MD simulations. Corrections to the ideal gas phenomenology will involve accounting for the effects of interactions between the excitations. This may be easiest for the XY model, and will provide an instructive example for dealing with additional modifications due to in-plane anisotropy and due to other lattices, such as triangular and honeycomb.

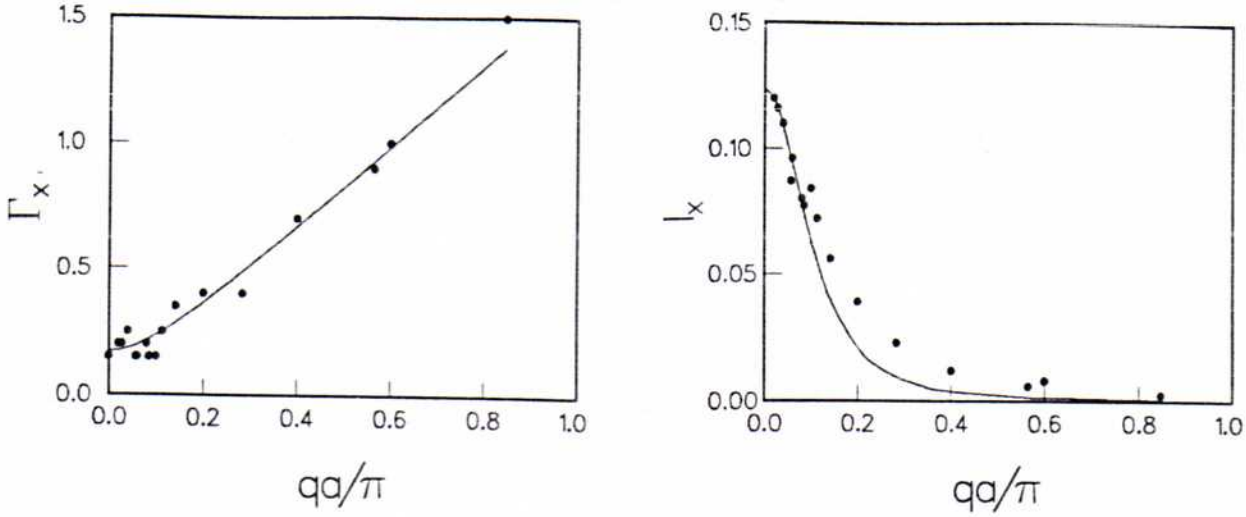

Fig. 6. Central peak properties of $S_{xx}(\vec{q},\omega)$ for the XY model at T = 1.0. In a) we show estimates of the CP width Γ_x from MC-MD data and compare with Eq. 26 using $\bar{u} = 0.9$ and $\xi = 3.0a$. In b) we show estimates of the CP intensity I_x from MC-MD data and compare with Eq. 27 using $\xi = 2.4a$.

REFERENCES

* Supported by CNPq (Brazil).

1. L. P. Regnault and J. Rossat-Mignod: In Magnetic Properties of Layered Transition Metal Compounds, eds., L. J. De Jongh and R. D. Willett (Reidel, Dordricht 1987).
2. M. T. Hutchings, J. Als-Nielsen, P. A. Lindgard, and P. J. Walker: J. Phys. C. 14, 5327 (1981).
3. M. Elahy and G. Dresselhaus: Phys. Rev. B30 7225 (1984).
4. J. M. Kosterlitz and D. J. Thouless: J. Phys. C. 6, 1181 (1973); Prog. Low Temp. Phys. Vol. VIIB, Chapter 5, ed. D. F. Brewer (North-Holland, Amsterdam 1978).
5. D. L. Huber: Phys. Lett. 76A, 406 (1980); Phys Rev. B26, 3758 (1982).
6. H. J. Mikeska: J. Phys. C 11, L29 (1978); J. Phys. C 13, 2313 (1980).
7. F. G. Mertens, A. R. Bishop, G. M. Wysin, and C. Kawabata: Phys. Rev. Lett. 59, 117 (1987).
8. C. Kawabata and A. R. Bishop: Sol. State Comm. 60, 169 (1986).
9. C. Kawabata, M. Takeuchi, and A. R. Bishop: J. Magn. Magn. Mat. 54-57., 871 (1986); J. Stat. Phys. 43, 869 (1986).
10. S. Hikami and T. Tsuneto: Prg. Theor. Phys. 63, 387 (1980).
11. Note that Eq. 3, 4, and 6 differ from the dynamic Eqs. of Ref. 10.